Electrical, magnetic and structural characterization of fullerene soots

1996 J. Phys.: Condens. Matter 8 2127

(http://iopscience.iop.org/0953-8984/8/13/005)

J. Phys.: Condens. Matter **8** (1996) 2127–2141. Printed in the UK

Electrical, magnetic and structural characterization of fullerene soots

L J Dunne†§, A K Sarkar†, H W Kroto†, J Munn‡, P Kathirgamanathan‖, U Heinen†, J Fernandez‖, J Hare†, D G Reid† and A D Clark§

† School of Chemistry and Molecular Sciences, University of Sussex, Falmer, Brighton BN1 9QJ, UK

‡ Electron Microscopy Unit, Department of Crystallography, Birkbeck College, University of London, Malet Street, London WC1, UK

§ School of Applied Science, South Bank University, London SE1 0AA, UK

‖ School of Electrical and Electronic Engineering, South Bank University, London SE1 0AA, UK

Received 30 October 1995, in final form 11 January 1996

Abstract. Although it is some five years since fullerenes were extracted in macroscopic quantities from the black, superficially amorphous sooty deposits produced by a carbon arc under helium, little is known in detail about the structure of the deposit or its electrical and magnetic properties. Here we provide evidence that this deposit, known as fullerene soot, is composed of defective networks of carbon atoms which do not have all valencies satisfied. We have studied these soots, before and after thermal annealing, using x-ray and electron diffraction, electron spin-resonance (ESR) spectroscopy, infra-red transmission and measurements of electrical conductivity. We find that localized states associated with such dangling bonds are removed from the soot on annealing and this process is accompanied by an ordering transition which modifies the electrical and magnetic properties. The fullerene soot particles appear to be encapsulated aggregates of highly defective carbon 'onions'. Such metastable defective networks undergo a subtle ordering processes upon heat treatment which is accompanied by a rise in the electrical conductivity and a loss of paramagnetism due to the elimination of unsatisfied carbon atom valencies. Electrical conductivity and infra-red transmission measurements indicate that the centre of these 'onions' is graphitic, with metallic properties. The temperature dependence of the electrical conductivity suggests that charge transport in both annealed and unannealed materials occurs by tunnelling between metallic islands in the sample. The ESR linewidth, arising from the spin centres in fullerene soots, is not significantly changed by exposure to oxygen. This suggests that the free radical centres in fullerene soots are extremely efficiently isolated from the atmosphere—presumably by encapsulation. This behaviour contrasts with that of amorphous carbons prepared by thermal decomposition of organic materials (chars). The ESR g-factors of the fullerene soots are lower than those of chars, which suggests that the radicals in fullerene soots have strong sigma character due to unsatisfied sp^2-type valencies. In this paper, a plausible structure and associated annealing mechanism for the fullerene soot is presented based on these experimental observations.

1. Introduction

A fascinating solid black condensate (here called fullerene soot) is generated in the gas phase and deposited during the discharge in a Krätschmer–Huffman carbon arc fullerene generator [1]. Following the work of Krätschmer *et al* and many other subsequent studies [1–7] it is now known that this form of pure carbon typically contains a few per cent of

0953-8984/96/132127+15$19.50

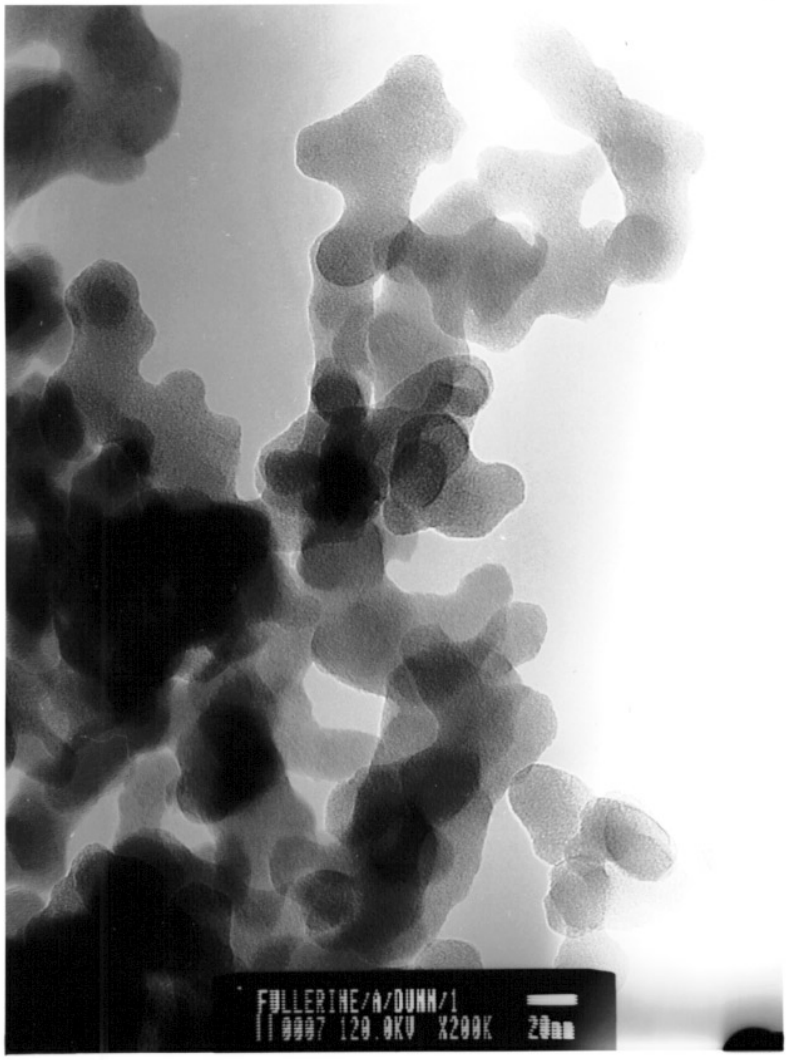

Figure 1. Small-aperture transmission electron diffraction of 50 Torr He soot. The spot pattern shown is consistent with a collection of randomly orientated graphitic microcrystallites as shown in figure 3.

extractable fullerenes of which C_{60} is dominant. Although publications dealing with novel aspects of fullerenes abound, less is known about the nature of fullerene soot. In this paper a summary of the results of an extensive structural, electrical and magnetic characterization of fullerene soot is presented and a comparison is made with the data obtained after annealing the material. Several studies which have focused mainly on electron microscope studies of the fullerene soot have appeared [3, 6–8] but here we focus on the annealing process and relate the structural changes observed by electron microscopy to changes in electrical and magnetic properties. The characterization of the annealing transition has been implemented with the aid of ESR spectroscopy, optical absorption measurements, high-resolution transmission electron microscopy (HRTEM) and electrical conductivity as well

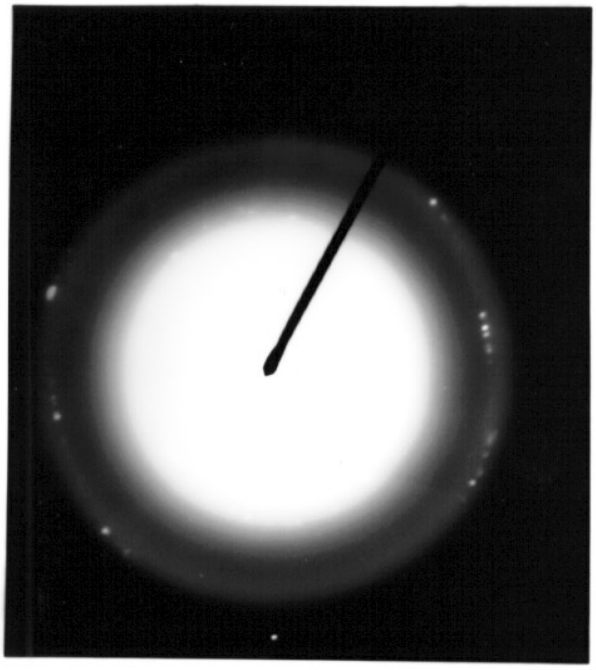

Figure 2. A transmission electron micrograph of 50 Torr He fullerene soot showing coagulated balloons which are suggested to be sealed containers of defective free radical material. Notice that the shape of the particles suggests that the balloons contain several structures held together initially by Van der Waals forces and then sealed by a number of coats of carbon atoms in the gas phase.

as Hall coefficient measurements. ESR and electron diffraction measurements show that the annealed soots are more ordered than the nascent fullerene soots. The key result is that on annealing, the localized component of the ESR signal disappears with a concurrent rise in electrical conductivity resulting from an increased connectivity of the structure. These changes are accompanied by simultaneous changes in the electron micrograph patterns and x-ray diffraction profiles which enable us to propose plausible structural characteristics for the fullerene soot and to rationalize the changes in electrical and magnetic properties induced by annealing.

2. Fullerene soot preparation and structural characterization

The fullerene soot used in this study was prepared using the now standard Krätschmer–Huffman technique [1]. Helium was used as the quenching gas at a pressure of 50 Torr. For annealing, the soot samples were placed in quartz boats which were then loaded into a pyrolysis tube and heated at 1273 K under flowing argon at atmospheric pressure. The heat treatment was applied for seven hours after which time the samples were allowed to cool (under argon flow). Whereas the original soot is very loose and light, the annealed soot is much more compact.

An electron micrograph, taken using a JEOL 1200EX electron microscope operating at 120 keV, of an unannealed fullerene soot is shown in figure 1 where it can be seen that the soot is made up of irregularly shaped balloons of typical lateral dimensions around 50 nm.

During the discharge of a carbon arc, highly defective carbon 'onions' of different sizes will form via an icospiral mechanism [28]. Gas-phase aggregation of such large polarizable 'onion' structures is also expected. The coagulation of fullerene soot particles has been observed previously by Ugarte [3, 6, 7] and our micrographs are similar in form to those reported by him for soots prepared at 100 Torr He pressure. We believe that the shape of the fullerene soot particles is that of encapsulated aggregates or sealed bags of these carbon 'onions'.

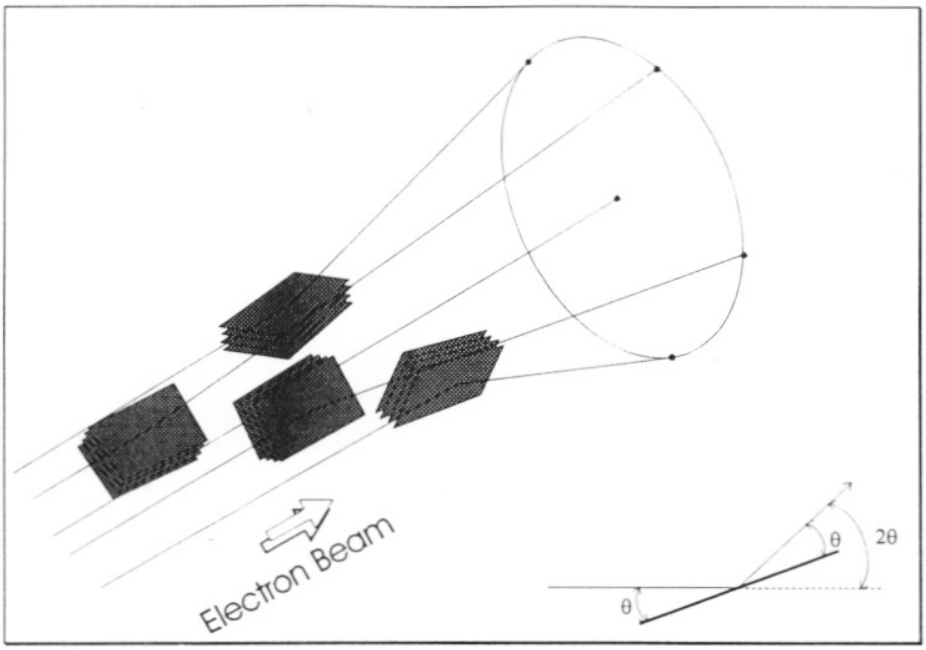

Figure 3. A possible origin of the random spot pattern in figure 2.

We have succeeded in capturing on film (figure 2) evidence for polycrystalline regions in the unannealed soots. Selected-area electron diffraction indicates that the fullerene soot is in large part amorphous; however, an extensive search showed regions with randomly arranged spot diffraction patterns, indicating the existence of randomly oriented graphitic microcrystallites in the material. A possible structural interpretation (figure 3) of the origin of such a spot pattern is that it arises from graphitic microcrystallites embedded in the unannealed soot. The corresponding x-ray diffraction profile of the unannealed material gave a main reflection with a spacing of 3.34 Å which is very close in position to the (002) reflection in graphite [10, 11] in agreement with the work of others [9]. However, the x-ray diffraction peak is broad which is indicative of very small crystallites. The electron diffraction studies indicate that these cannot be larger than about 100 Å.

On annealing, the individual peaks in the x-ray diffraction profile become narrower indicating that the annealed material has formed more extended regions of order which is consistent with the images seen in the electron micrographs. The 100 Torr fullerene soot studied by Ugarte [3, 6, 7], when annealed at ∼2000 K for one hour, undergoes a spectacular structural transformation. Figures 4–6 show some typical transmission electron micrographs

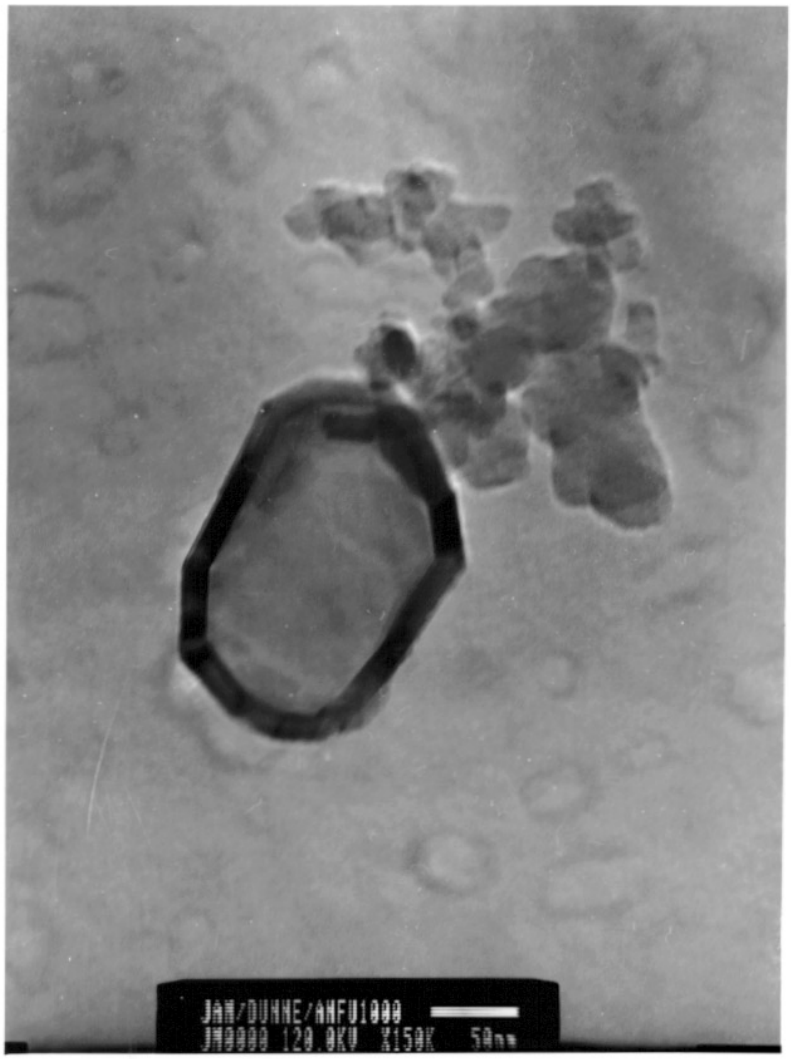

Figure 4. The nanoparticle formed on annealing the 50 Torr He soot (seven hours at 1273 K in flowing argon).

(TEMs) obtained after annealing our 50 Torr fullerene soot at 1273 K for seven hours. The annealed material is inhomogeneous and contains regions with submicron-sized particles as shown in figure 4, disordered regions and partially crystalline regions as shown in figure 5, which captures an intermediate stage in the formation of a nanotube. Figure 6 shows nanostructures contained in the interior of other submicron-sized structures suggesting that collapse of the material on the inside of the balloon-like structures occurs on annealing. It can be seen from the presence of inner walls in the tube that collapse of the walls between coagulated particles occurs at a late stage. Figure 7 shows selected-area electron diffraction from the annealed soot clearly showing crystalline regions. (See also figure 8.)

The structure for the unannealed soot which best fits the electron and x-ray diffraction data is that of a defective arrangement of small fragments containing several planar or

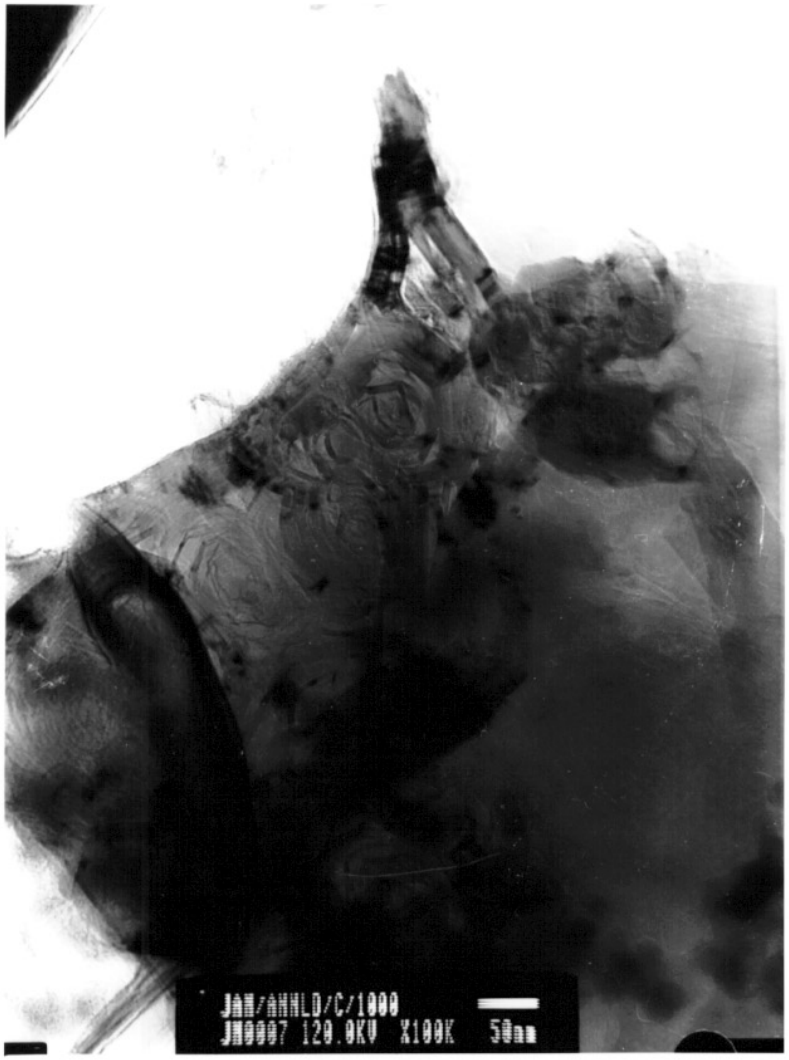

Figure 5. A section of an open tube formed on annealing the 50 Torr He soot (seven hours at 1273 K in flowing argon).

non-planar layers of carbon atoms. It is unlikely that, during the gas-phase formation of fullerene soots, the edge atoms in defective carbon layers can satisfy all valencies and hence it is expected as we verify below that the balloons are essentially sealed containers with free-radical-containing material inside. This suggestion is supported by ESR measurements as described below.

3. Electron spin-resonance (ESR) investigations

The ESR absorption measurements on the fullerene soot samples were measured on a Bruker ESP 300 ESR spectrometer operating at X-band and at 5 mW microwave power to avoid saturation. Figure 9 depicts a set of typical ESR lineshapes obtained from a fullerene soot

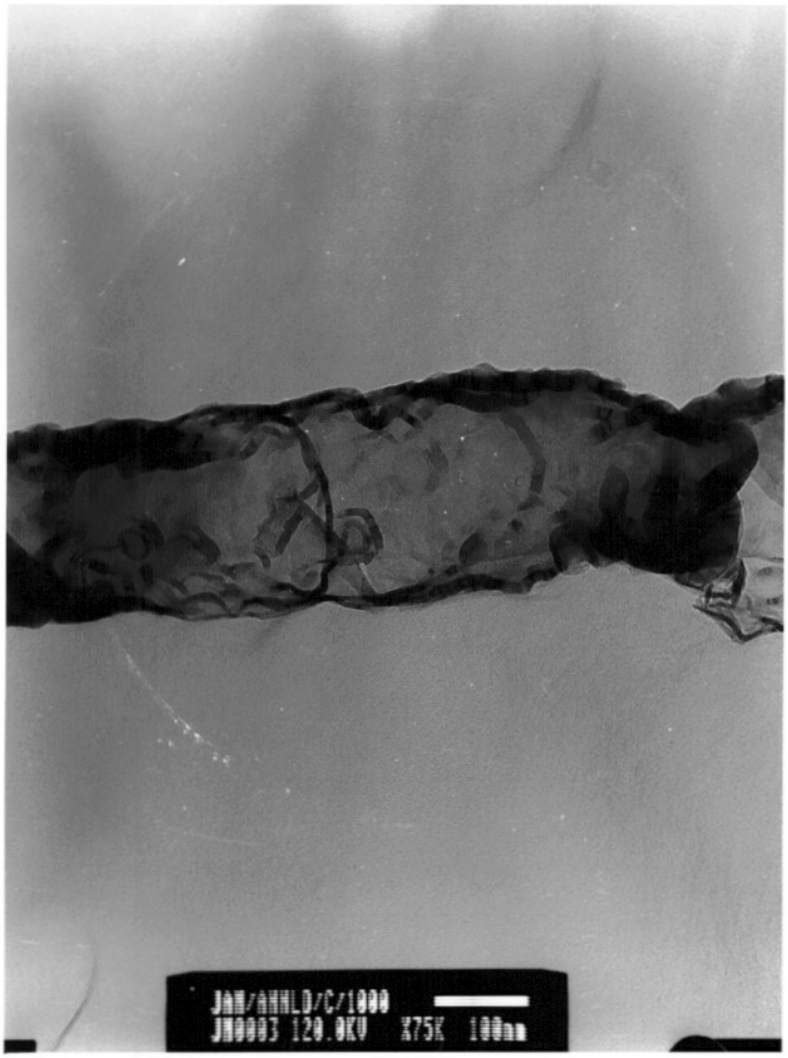

Figure 6. Partial formation of a nanotube formed by annealing 50 Torr He soot (seven hours at 1273 K in flowing argon). Note the disordered material and wall in the interior of the tube.

sample (i) in air at 300 K, and (ii) in vacuum at 300 K. All of the signals recorded were symmetric; this contrasts with the asymmetric lineshapes that have been observed from polycrystalline graphites where the resonance is due to conduction electrons [12, 13].

The temperature dependence of the ESR signal is shown in figure 10. The intensity decreases by approximately a factor of two over the temperature range 100 K to 300 K whereas a factor of three would be expected from Curie's law. This indicates the presence of localized spins whose intensity follows Curie's law but, in addition to explain this deviation from Curie's law, a tentative explanation, consistent with the our overall structural viewpoint, is the presence of a thermally activated component consistent with a singlet–triplet transition. A straightforward analysis [14] yields an estimate of the spin concentration of both components of very roughly 10^{21} g^{-1} which corresponds to approximately 1 spin

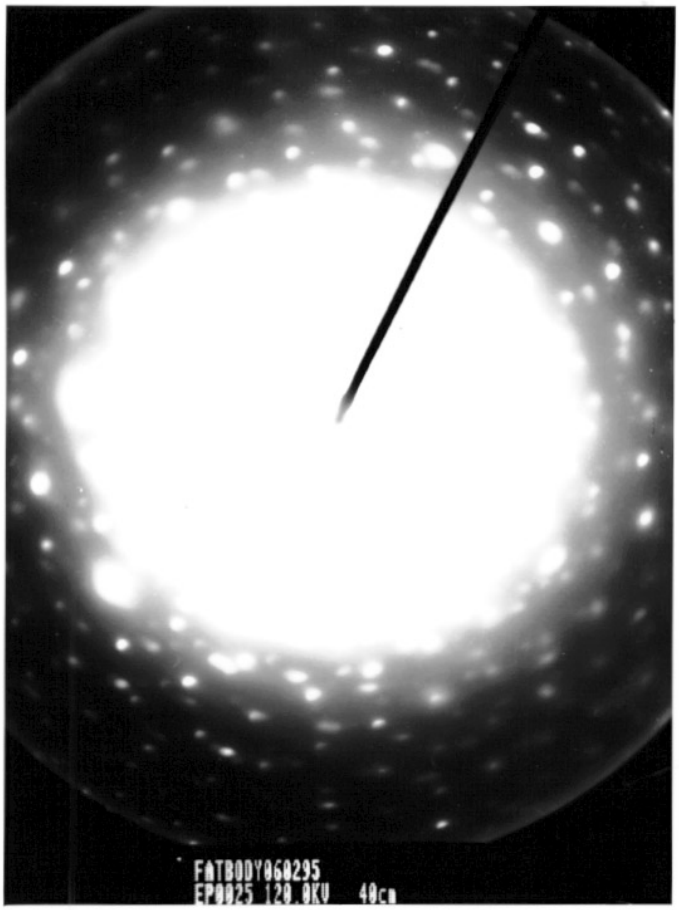

Figure 7. Small-aperture transmission electron diffraction from annealed fullerene soot indicative of quasi-crystalline order in small regions of the annealed (seven hours at 1273 K in flowing argon) 50 Torr He fullerene soot. The exact atomic arrangement responsible for the pattern is not known.

for every 10–100 carbon atoms. The singlet–triplet splitting was estimated to be 0.03 eV. Since it is expected, as supported by results described below, that the unannealed fullerene soots are essentially sealed containers with free radical material inside, we attribute the ESR signals to unsatisfied valencies at the edges of carbon fragments in the interior. Spin centres which are close in space may couple to give a non-magnetic singlet ground state which may be thermally activated to a triplet state. The ESR g-factor for the fullerene soot before annealing in the temperature range 100–300 K is close to 2.0023 and the peak-to-peak linewidth was close to 2×10^{-4} T over the same temperature range. By contrast, the ESR linewidth in graphite rises with an approximately inverse temperature dependence indicating that the spin centres in fullerene soots are of a quite different origin from those in standard graphites [12].

In amorphous carbons, prepared by the thermal decomposition of organic materials, paramagnetic centres which give rise to ESR signals can be observed at the onset of charring [14–18]. An analysis of the g-factors for a range of chars [17] indicates that

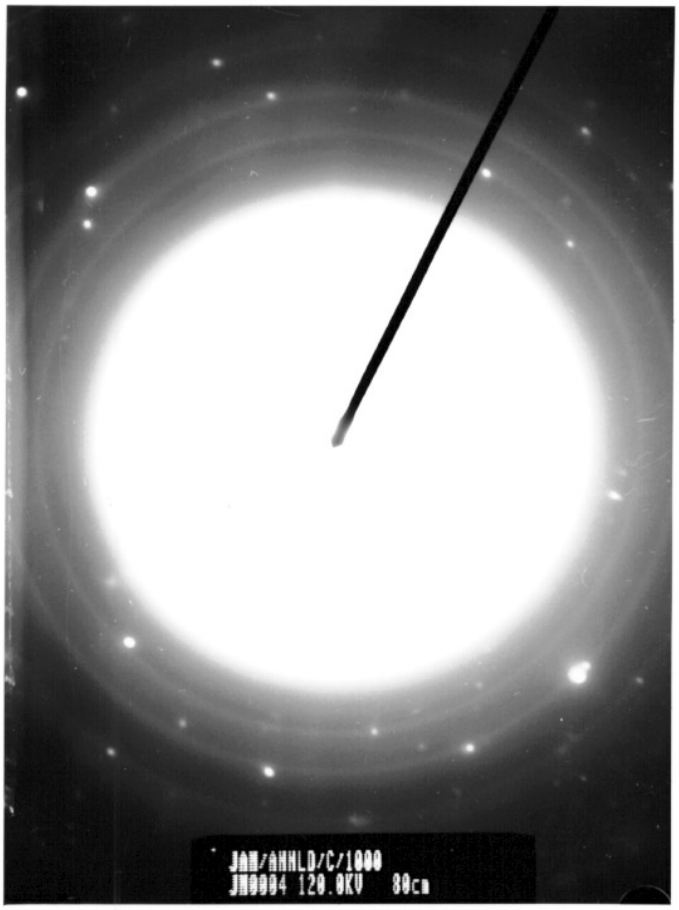

Figure 8. As figure 7.

these are typically in the range of values 2.0030–2.0034, consistent with odd-alternant π-radical carriers. Hence it appears that the radicals in fullerene soots and chars are not of the same type. In marked contrast to those of chars [15–18], the linewidths of the fullerene soot resonances did not change to any significant degree when the samples were exposed to oxygen (figure 11). In chars, the interaction with paramagnetic oxygen molecules causes a dramatic broadening effect. The absence of such an oxygen effect is significant since it indicates that the spin centres in the fullerene soot are inaccessible to the paramagnetic oxygen molecules which are likely to cause dipolar broadening of the ESR absorption [19]. A plausible explanation is that in fullerene soots, the free radicals are encapsulated.

On the other hand the annealed soot, prepared at 50 Torr He pressure, did not show ESR signals which is consistent with the complete satisfaction of free valencies during structural rearrangements caused by annealing as discussed above. It is possible that ESR activity in the annealed fullerene soot has remained undetected due to relaxation effects, such as collisions with impurities or with the edges of crystallite, which have broadened the resonances beyond detection. Charge-carrier ESR absorption has been observed in nanotubes with quite similar characteristics to the ESR absorption in graphite [20]. In

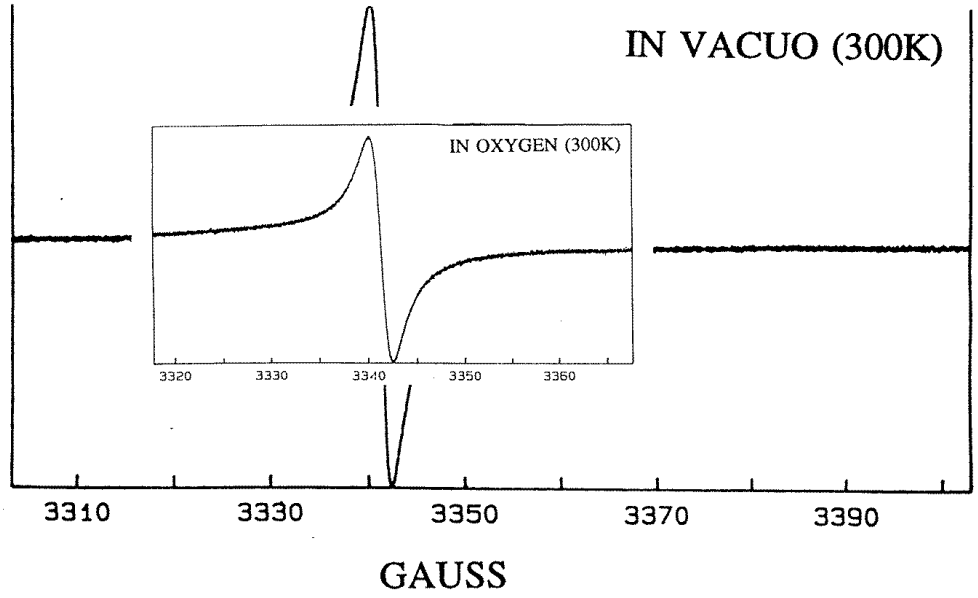

Figure 9. Typical ESR spectra of unannealed fullerene soot.

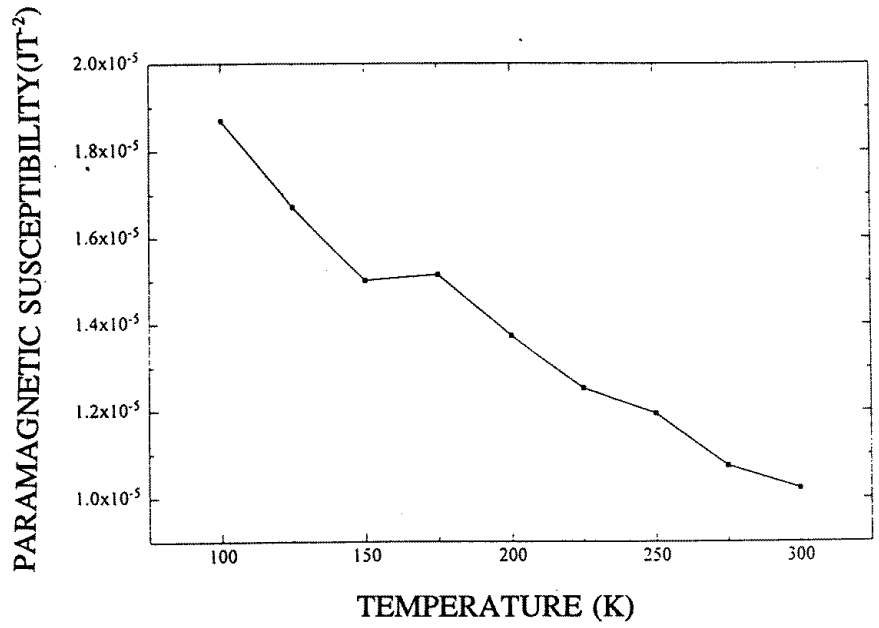

Figure 10. The temperature dependence of the paramagnetic susceptibility of fullerene soots.

some fullerene soots annealed under different conditions an ESR signal with very weak temperature-dependent intensity has been observed which is characteristic of charge-carrier Pauli paramagnetism.

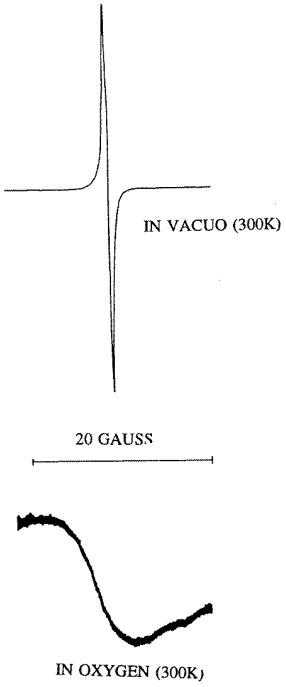

Figure 11. The oxygen effect in the ESR absorption signal measured at 300 K obtained from a amorphous carbon char (sulphanilic acid) decomposed in argon at 900 K described in detail in [18]. Note that the signal broadens by a factor of about 20 on exposure to oxygen suggesting that the spin centres are exposed to paramagnetic oxygen molecules. No such effect is observed in fullerene soots.

4. Electrical conductivity measurements

Electrical conductivity measurements were carried out on discs of fullerene soot compacted with polyvinyl chloride (PVC) as a binder (binder concentration 15% by mass), by the Van der Pauw method [21]. The conductivity, at room temperature, of an unannealed sample is 5×10^{-6} S cm^{-1} and that of an annealed sample is 2×10^{-5} S cm^{-1}. The compaction was carried out at 1248 kg cm^{-2}. The conductivity as a function of temperature, $\sigma(T)$, was thermally activated and found to give a good fit (the correlation coefficients are 0.995 and 0.984 for unannealed and annealed samples respectively) to the form

$$\sigma(T) = \sigma_0 \exp(-bT^{-1/2}) \tag{1}$$

as shown in figure 12. Such a functional form for the temperature dependence of the electrical resistance is characteristic of percolation charge carriers tunnelling through a matrix of conducting particles [22, 23]. We should point out that a plot of $\ln(\sigma)$ versus $1/T$ is also roughly linear (correlation coefficients are 0.974 for both unannealed and annealed samples), but the correlation is inferior to that of the fit proposed above.

It is noteworthy that the slopes of the plots in figure 12 are unaffected by the annealing process. In a percolation process charge carriers seek pathways offering minimum resistance. Qualitatively it would appear that similar pathways exist in both materials but that the concentration of these in the annealed samples is higher.

The conductivity for the unannealed sample, extrapolated to infinite temperature, is 5.5×10^{-4} S cm^{-1} which is consistent with a mechanism involving tunnelling or hopping between localized states [26]. For the annealed soot the corresponding value is 2.8×10^{-3} S cm^{-1}. Hall mobility measurements indicate that the charge carriers are holes with densities of $\sim 1.4 \times 10^{18}$ m^{-3} for the unannealed sample and $\sim 2.6 \times 10^{19}$ m^{-3} for the annealed sample. It is useful to compare these values with ambient temperature conductivity

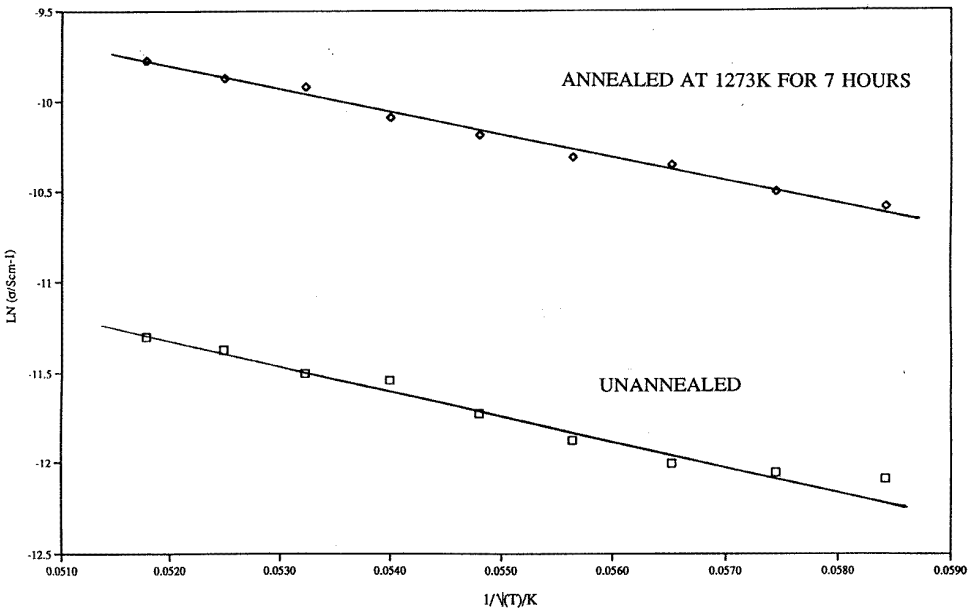

Figure 12. The temperature dependence of the electrical conductivities of unannealed and annealed (seven hours at 1273 K in flowing argon) fullerene soot showing an activated conduction of the form $\sigma(T) = \sigma_0 \exp(-bT^{-1/2})$ indicative of tunnelling between metallic islands in the materials.

($\sim$730 S cm^{-1}) and the charge-carrier density ($\sim 3 \times 10^{24}$ m^{-3}) for semi-metallic graphite [24, 25]. These increased values reflect the significantly higher structural order in extended graphitic material. The mobility values are 2.25×10^{-3} m^2 V^{-1} s^{-1} for the unannealed sample and 4.9×10^{-4} m^2 V^{-1} s^{-1} for the annealed sample. These mobility values are too large to be associated with carriers hopping below a mobility edge [26] and it seems more likely that the carrier wavefunctions are only very weakly localized. The conductivities of both the annealed and the unannealed samples are roughly independent of frequency up to $\sim$10 MHz. The rise in conductivity in this high-frequency region is highly suggestive of hopping/tunnelling between conductive islands in these materials. The capacitance of the unannealed sample was measurable but that of the annealed sample was too lossy to allow comparison. This behaviour is indicative of a large increase in the concentration of metallic regions in the annealed material.

The electrical conductivity studies reported here have yet to be explained by a detailed theoretical model but they are consistent with carriers which tunnel between conductive islands. The conductive islands are presumably graphitic and from the carrier densities the concentration of such ordered graphitic regions rises by about a factor of ten on annealing. We do not find any evidence for a contribution to the conductivity from localized spins and indeed electrons in σ-bonds have very low electrical mobilities. Indeed, the very fact that electron spin-resonance absorption is observed in the unannealed fullerene soots suggests that electrons in σ-bonds are Anderson–Mott–Hubbard localized [26].

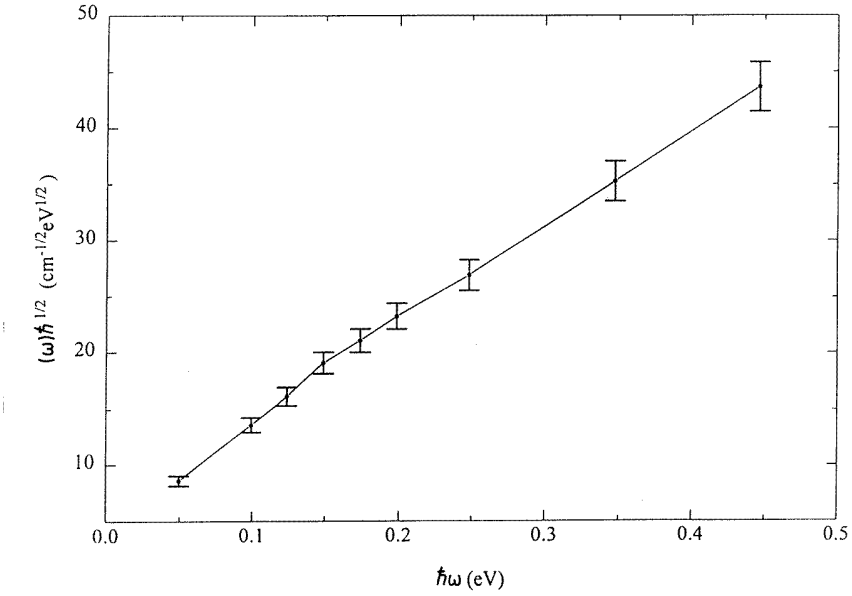

Figure 13. A plot of $(\alpha(\omega)\hbar\omega)^{1/2}$ against photon energy for a thin film of fullerene soot prepared at a pressure of 50 Torr He.

5. Infra-red transmission measurements

In electrically conducting solids with small band gaps, infra-red absorption due to electronic transitions may be observed. In many crystalline semiconductors an optical absorption edge enables the band gap to be determined spectrometrically. Many amorphous semiconductors show frequency- (ω-) dependent optical absorption $\alpha(\omega)$ of the power-law form given by [18, 26]

$$\alpha(\omega) = K(\hbar\omega - \hbar\omega_0)^n/\hbar\omega \tag{2}$$

where K is a constant and n is usually in the range 1–3. $\hbar\omega_0$ is the lowest energy gap for electronic transitions. This procedure allows a band gap to be measured optically. In figure 13 the unannealed fullerene soots are shown to follow the above law quite well when $n = 2$. It is evident that the plot is linear and, subject to the small experimental errors, extrapolates through the origin. The implication of this observation is that it strongly supports the notion that fullerene soots contain metallic islands which are likely to be due to extended layers of carbon atoms containing delocalized electronic states. The optical absorption and electrical conductivity of the unannealed fullerene soots are consistent with the conclusion drawn from the electrical conductivity measurements above that the conductivity is due to tunnelling between metallic islands with zero optical gap in the material.

6. Discussion

On the basis of the evidence presented above we are now able to make some inferences about the structure of fullerene soots. Fullerene soots are formed by nucleation of a carbon

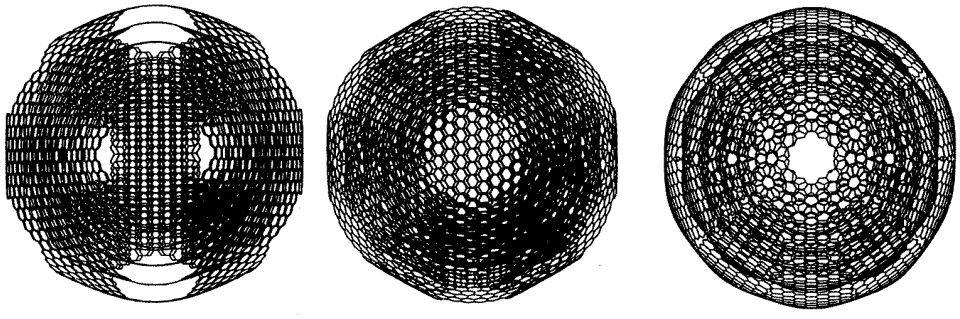

Figure 14. Suggested structure of typical contents in the interior of an unannealed fullerene soot particle. A defective carbon 'onion' with dangling bonds is shown from several viewpoints. The balloon-type structures shown in figure 1 are thought to be effectively sealed containers of such defective metallic 'onions' [29].

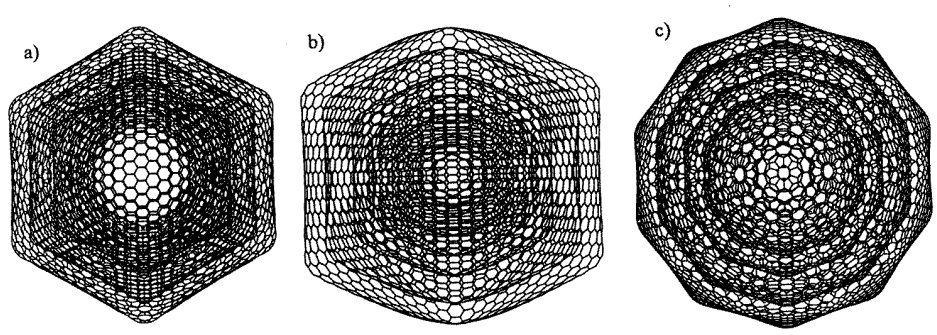

Figure 15. A perfect nanoparticle seen from several viewpoints.

plasma. However, little is known about the detailed mechanism of the process. The studies described here can be rationalized if the interiors of unannealed fullerene soots are composed of characteristic structures similar to those shown in figure 14 in which carbon layers contain voids or defects at a level which is consistent with the ESR result—namely $\sim$1 spin per 10 carbon atoms. The bonds at the edges of the defects, so-called dangling bonds, appear to give rise to the experimentally observed ESR signals. Spin centres which are in close proximity may couple in pairs to give triplet states, thereby accounting semi-quantitatively for the temperature dependence of the ESR signals in the unannealed soots. The lack of any observable effect of oxygen in the ESR spectra of the unannealed soot together with the TEM images indicates that the spin-carrier phase is encapsulated inside effectively closed carbon cages. It seems unlikely that the interior of the soot particle is entirely covalently bonded. During the gas-phase formation of such carbon structures, aggregation may occur by van der Waals interactions which will be strong between such essentially metallic molecules with large polarizabilities.

On annealing, it appears that several processes occur, all involving the removal of the defect voids in the defective carbon 'onions'. One such process involves the removal of defective layers in the interior of an 'onion' structure to form the nanoparticle shown in figure 15. The rise in the conductivity on annealing is attributed to an increasing

concentration of metallic islands in the material. The annealing process studied here appears to involve the removal of the walls of the coagulated unannealed particles to produce a new form of nanostructured material. The driving force for the annealing process is the need for unstable defective carbon networks to eliminate the large number of dangling bonds trapped at defect sites in carbon sheets by the most expedient locally accessible network-extending process [27].

Acknowledgments

It is a pleasure to thank Professors J N Murrell, P Nolan and W Blau, and Dr Conor O'Carroll for helpful comments.

References

[1] Kratschmer W, Lamb L, Foristopoulos K and Huffman D 1990 *Nature* **347** 354
[2] Kroto H W, Heath J R, O'Brien S C, Curl R F and Smalley R E 1985 *Nature* **318** 162
[3] Ugarte D 1994 *Carbon* **32** 1245
[4] Iijima S 1991 *Nature* **354** 56
[5] Iijima S 1980 *J. Cryst. Growth* **50** 675
[6] Ugarte D 1992 *Chem. Phys. Lett.* **198** 596
[7] Ugarte D 1992 *Nature* **359** 707
[8] Miki-Yoshida M, Castillo R, Ramos S, Rendon L, Tehuacanero S, Zou B S and Jose-Yacaman M 1994 *Carbon* **32** 231
[9] Werner H, Herein D, Blocker J, Henschke B, Tegtmeyer U, Schedel-Niedrig T, Keil M, Bradshaw A M and Schlogl R 1992 *Chem. Phys. Lett.* **194** 62
[10] Biscoe J and Warren B E 1941 *J. Appl. Phys.* **9** 492
[11] Ergun S 1968 *Chemistry and Physics of Carbon* vol 3 (New York: Dekker) p 211
[12] Singer L S and Wagoner G 1962 *J. Chem. Phys.* **37** 1812
[13] Dyson F J 1955 *Phys. Rev.* **98** 349
[14] O'Reilly D E and Anderson J H 1965 *Chemistry and Physics of the Organic Solid State* vol 2, ed D Fox, M M Labes and A Weissberger (New York: Interscience) p 120
[15] Ingram D J E 1958 *Free Radical as Studied by Electron Spin Resonance* (London: Butterworth)
[16] Lewis I C and Singer L S 1981 *Chem. Phys. Carbon* **17** 1
[17] Dunne L J, Clark A D, Chaplin M F and Katbamna H 1992 *Carbon* **30** 1227
[18] Roulston S A, Dunne L J, Clark A D and Chaplin M F 1990 *Phil. Mag.* B **62** 243
[19] Singer L S 1963 *Proc. 5th Carbon Conf. (Buffalo, 1962)* vol 2 (Oxford: Pergamon) p 37
[20] Kosaka M, Ebbesen T W, Hiura H and Tanigaki K 1995 *Chem. Phys. Lett.* **233** 47
[21] Van der Pauw L J 1958 *Philips Res. Rep.* **13** 1
[22] Sheng P, Abeles B and Arie Y 1973 *Phys. Rev. Lett.* **31** 44
[23] Abeles B, Sheng P, Arie Y and Coutts M 1975 *Adv. Phys.* **24** 407
[24] Burns G 1985 *Solid State Physics* (London: Academic) p 340
[25] *Handbook of Chemistry and Physics* 1987–1988 68th edn, ed R C Weast (Boca Raton, FL: Chemical Rubber Company Press)
[26] Mott N F and Davis E A 1971 *Electronic Processes in Non-Crystalline Materials* (Oxford: Clarendon)
[27] Zhang Q L, O'Brien S C, Heath J R, Liu Y, Kroto H W and Smalley R E 1986 *J. Phys. Chem.* **90** 525
[28] Kroto H W and McKay K G 1988 *Nature* **331** 321
[29] Sarkar A 1994 *PhD Thesis* University of Sussex